Microstructural and mechanical characterisation of 5XXX-H111 friction stir welded tailored blanks

A. Tronci[1,2], R. McKenzie[1,3], R. M. Leal[1,4] and D. M. Rodrigues*[1]

Friction stir welds in 1 mm thick plates of AA 5182-H111 and AA 5083-H111 aluminium alloys are analysed in this paper. The welds were produced using a large range of welding conditions, namely, different process control modes (position and load control), tool parameters (different geometries and dimensions) and process parameters (rotation speed, advancing speed and axial load). Visual inspection and metallographic and mechanical analysis demonstrate that it is possible to obtain consistently good quality welds in very thin plates under a large range of welding conditions. Important relations between base material properties, tool geometry and the final properties of the welds were established.

Keywords: Aluminium alloys, Thin plates, Friction stir welding, Microstructure, Mechanical properties

Introduction

Friction stir welding (FSW) has been the object of investigation by several research groups during the last decade.[1,2] Although this process can be used to join several materials such as magnesium, copper, steel, titanium and metal matrix composites, the primary research and industrial interest for this process were for butt and lap joining of aluminium alloys, especially for the 2XXX, 6XXX and 7XXX series of heat treatable aluminium alloys, usually considered to be unweldable by fusion welding processes. Research in this field is still very intense,[3–6] and may be for this reason, FSW of the AA 5XXX series of aluminium alloys is substantially less explored. However, from the published literature it can be concluded that the mechanical properties of the welds produced from AA 5XXX alloys depend mainly on the grain size and on the dislocation density due to plastic deformation and recrystallisation occurring during welding.[7–11] In this way, when the AA 5XXX alloy series are welded in the annealed condition, no softening occurs in the thermomechanically affected zone (TMAZ) and heat affected zone. In contrast, when these alloys are welded in the strain hardened condition, the work hardened structure will readily recover and/or recrystallise during welding, and softening may occur.

Among the AA 5XXX series of aluminium alloys, the FSW of AA 5083 is the most studied, either in similar[12–22] and dissimilar[23,24] welding combinations.

Some efforts were also put to study the FSW of the AA 5754,[25] AA 5052,[26–28] AA 5456,[29,30] AA 5251,[31,32] AA 5182[33] and AA 5086[34,35] series of alloys. Some of these authors analysed the influence of the rotating speed,[25,27] the advancing speed,[12,34] both of these factors together[15,18,19] and even the interaction of tool's geometry with these parameters[12,19,25] on weld quality. However, despite the huge interest of the AA 5XXX alloys in automotive construction, where this type of alloy is extensively applied in the production of very thin plate panels, in most of above studies the thickness of the plates was >5 mm and only one of them focused on FSW of plates less than 2 mm thick.[33] As a matter of fact, obtaining non-defective welds in very thin plates, with excellent surface finishing and plastic properties, which makes them able to be processed by plastic deformation, represents an additional challenge in the application of the FSW process.

Another important aspect in FSW process development is to guarantee improved levels of welding productivity. Since in any welding operation, in an industrial context, the welding speed has a direct influence on the process productivity, one of the main criteria in the selection of suitable welding parameters has to be the maximisation of the welding speed while ensuring acceptable welding quality. Owing to the huge interest of the AA 5XXX alloys in automotive industry, the influence of the base material properties and a large range of welding conditions, which included varying welding speeds, on the mechanical and microstructural properties of welds in very thin plates was analysed.

Material and methods

The base materials used in this investigation were AA 5182-H111 and AA 5083-H111 non-heat treatable aluminium alloys. As shown in Fig. 1, the 1 mm thick

[1]CEMUC, Department of Mechanical Engineering, University of Coimbra, 3030-788 Coimbra, Portugal
[2]Department of Mechanical Engineering, University of Cagliari, 40-09124 Cagliari, Italy
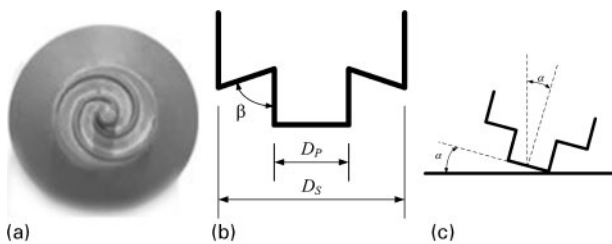[3]Department of Mechanical Engineering, Technological University of Panama, Panama City, Panama
[4]ESAD.CR, Polytechnic Institute of Leiria, Caldas da Rainha, Portugal

*Corresponding author, email dulce.rodrigues@dem.uc.pt
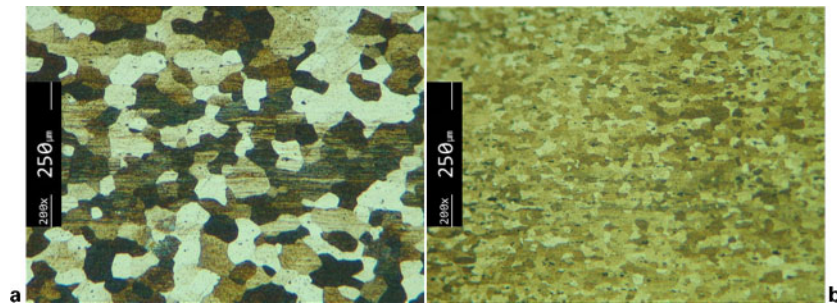
1 *a* AA 5182 and *b* AA 5083 base material microstructure

2 Friction stir welding tool

base material plates had a recrystallised microstructure with approximately equiaxed grains and relatively uniform grain sizes of 36 and 18 μm for the AA 5182 and AA 5083 alloys respectively.

Welds were produced from the base materials using a large range of welding conditions, which included different process control modes (position and load control), tool parameters (different geometries and dimensions) and process parameters (rotation speed, advancing speed and axial load). The tool parameters, which included varying geometries and shoulder dimensions (Fig. 2), are listed in Table 1. As shown in the table, the AA 5182 welds were produced using two different tools, a scrolled shoulder tool (Fig. 2*a*) and a conical shoulder tool ($\beta=82°$, Fig. 2*b*), and the AA 5083 welds were produced using flat ($\beta=90°$, Fig. 2*b*) and conical shoulder tools ($\beta=87°$, Fig. 2*b*). As shown in Fig. 2*a*, the scrolled shoulder had two helical flutes that forced material flow around the pin, enabling to work without the tool tilt angle ($\alpha=0°$, Fig. 2*c*). Independent of the geometry and dimensions, all the tools had a cylindrical threaded pin with 3 mm in diameter. In Table 1, the tools are identified using a two digit acronym where the first digit identify the shoulder geometry (C for conical, S for scrolled and F for flat) and the second digit identify the shoulder diameter.

The process parameters used in the tests are listed in Table 2. Some AA 5182 weldings were performed in position control in a milling machine, using the C10 and S14 tools and moving the tool at different travelling

speeds (160 and 320 mm min^{-1} respectively) and rotational speeds (1800 and 1120 rev min^{-1} respectively). Other AA 5182 weldings were performed in load control, using an ESAB LEGIO equipment and the S14 tool, with the same welding conditions of the position control welding (1120 rev min^{-1}, 320 mm min^{-1}) and also at increasing traverse speeds (480 and 640 mm min^{-1}).

The AA 5083 plates were joined in force control using the ESAB LEGIO equipment and the C10, C14 and F14 tools. Two different rotation speeds (750 and 1000 rev min^{-1}) and welding speeds (160 and 250 mm min^{-1}) were used. The axial loads for each tool were determined by performing preliminary tests in position control, identifying 650 kgf for S14 tool, 350 kgf for C10 tool and 700 kgf for C14 and F14 tools. In Table 2, the welds are identified using X–Y–Z acronym, in which X defines the type of tool used, Y defines the rotation speed and Z defines the traverse speed. The AA 5182 welds, performed with similar welding parameters but different types of tool control, are distinguished by adding P (position control) and F (force control) to the acronym.

The heterogeneity in mechanical properties across the welds was evaluated by performing hardness measurements transverse to the welding direction, using a microhardness tester from Shimadzu, with 50 gf for the AA 5182 alloy and 200 gf for the AA 5083 alloy. The load holding time was 15 s in all cases and the hardness measurements were spaced at intervals of 0·25 mm. The welds were cross-sectioned and prepared following the standard procedures for optical microscopy, performed using a Zeiss HD 100 microscope, and transmission electron microscopy (TEM) analysis, performed using an electronic transmission microscope Jeol JEM-100S. Average grain sizes were determined by the linear intercept method.

Bending specimens were taken from the welds and tested to 180° with a curvature radius of 5 mm, in an Instron 4206 equipment. Transverse tensile specimens, with the weld centred in the gauge section, were also constructed. All the tensile tests were carried out at

Table 1 Tool parameters

| Base material | Tools ID | Shoulder | | Tool tilt angle/° |
		Geometry	Shoulder diameter/mm	
AA 5182	C10	Conical (8°)	10	2·5
	S14	Scrolled	14	0
AA 5083	F14	Flat	14	2
	C10	Conical (3°)	10	2
	C14	Conical (3°)	14	2
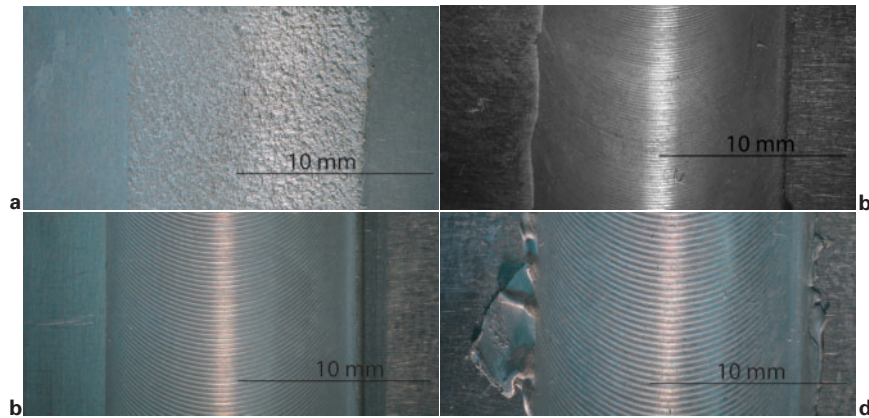
a S14-1120-320P; *b* F14-1000-160; *c* C14-1000-250; *d* C14-750-250
3 Weld crown appearance

room temperature on an autograph AG-X machine from Shimadzu using ARAMIS optical 3D deformation and strain measurement system for strain data acquisition, which enabled to access local stress–strain behaviour in the different sample regions.

Results

Visual inspection

Regardless of the large range of welding conditions tested in this work, the welds obtained for both base materials did not display any major structural defect. The weld crowns were regular in the welds produced with the scrolled shoulder (Fig. 3*a*), the flat shoulder (Fig. 3*b*) and the conical shoulders (Fig. 3*c* and *d*). As exemplified in Fig. 3*a*, all the welds produced with the scrolled tool had rough surfaces and were free of flash. Otherwise, the welds produced with the flat and conical tools (Fig. 3*b*–*d*), independent of the base material, displayed smooth surfaces with regularly spaced semi-circular bands. The presence of flash (Fig. 3*d*) was only observed in the AA 5083 welds produced at a low rotating speed (750 rev min^{-1}). Thickness under match relative to base plate's initial thickness was measured in the stirred zone of the welds performed with the C10, C14 and F14 tools. No thickness reduction across the stirred material was detected for the S14 welds, which were performed with 0° tilt angle. These results show a deep influence of tool geometry on weld morphology, being possible to conclude that the best surface finishing

was achieved with the flat and conical tools for the highest tool rotation speeds tested in this work.

Finally, the metallographic analysis and the bending tests revealed the presence of a very small and discontinuous kissing bond for the AA 5182 welds performed in force control, namely, the S14-1120-320F, S14-1120-480 and S14-1120-640 welds. Kissing bond was not detected for the welds performed in position control (S14-1120-320P), which indicates that the axial load used in the force control tests was insufficient to guarantee material flow under the pin.

Microstructural and mechanical analysis

The average grain sizes in the TMAZ (*d*), registered for the different welds, are shown in Table 3. Figure 4 shows the inverse of the square root of the TMAZ grain size ($\mu m^{-1/2}$) versus the tool rotation to traverse speed ratio (*W*/*v*) characteristics of each welding condition. Assuming that the temperature attained in the welding process increases with increasing *W*/*v* ratio, it is possible to conclude that, for the AA 5182 welds, the lower grain size values were obtained in the colder welding conditions (*W*/*v*<3·5), and the larger grain size values in the hotter welding conditions (*W*/*v*=11·0). It is also interesting to observe that for *W*/*v*<3·5, the grain size deeply varies with *W*/*v*, but for *W*/*v*>3·5, the grain size variation with *W*/*v* is less significant, which is in accordance with the hypothesis of a stabilisation of the heat generation in FSW with increasing tool rotation speeds.[36–38]

Table 2 Process parameters

Base material	Tools ID	Welds ID	*W*/rev min^{-1}	*v*/mm min^{-1}	*F*/kgf
AA 5182	C10	C10-1800-160	1800	160	Position control
	S14	S14-1120-320P	1120	320	
	S14	S14-1120-320F	1120	320	650
		S14-1120-480	1120	480	
		S14-1120-640	1120	640	
AA 5083	C10	C10-750-160		160	350
		C10-750-250	750	250	
		C10-1000-160		160	
		C10-1000-250	1000	250	
	C14	C14-750-160		160	700
		C14-750-250	750	250	
		C14-1000-160		160	
		C14-1000-250	1000	250	
	F14	F14-1000-160	1000	160	700
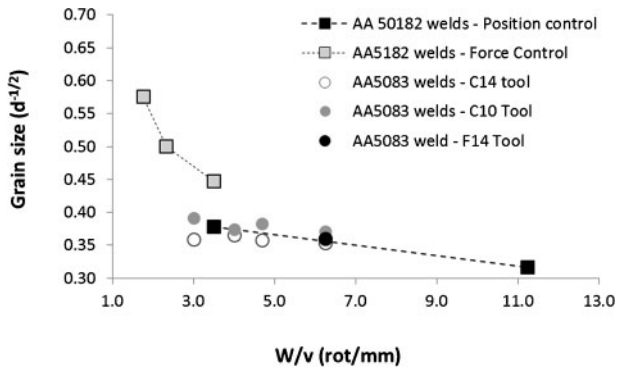
4 **Thermomechanically affected zone grain size ($\mu m^{-1/2}$) versus tool rotation to traverse speed ratio**

5 **Average weld hardness versus average grain size ($\mu m^{-1/2}$)**

The evolution of the recrystallised grain size for the AA 5182 welds, illustrated in Fig. 4, can be understood by analysing some of the factors influencing the recrystallisation kinetics, which include temperature, heating rate, strain, strain rate and the initial grain size of the base materials.[39] In fact, assuming that the rate of recrystallisation increases with strain and strain rate, it is possible to understand that the S14 welds, performed with a scrolled tool, which induce more intense plastic deformation on the stirred material than the C10 conical tool,[40] have lower recrystallised grain sizes than the C10 welds. In addition, it is also assumed that, according to the maximum temperature attained in the process, which increases with increasing tool rotation speed and decreasing traverse speed, static grain growth can take place after recrystallisation, which explains the occurrence of increasing grain size with increasing W/v ratio. It is also important to enhance that large grain size values were measured for the AA 5182 welds performed in position control (S14-1120-320P), when compared to that of the welds performed in load control under the same welding conditions (S14-1120-320F). Since the bending tests revealed the presence of kissing bond for the welds performed in load control, it is possible to assume that these welds were performed under a lower axial pressure than the welds performed in position control, which were free of any root defect. According to some authors,[41] the peak temperature in the welding process increases with increasing axial load, which explains the largest grain size values registered for the S14-1120-320P welds.

Analysing now the results in Fig. 4 relative to the AA 5083 welds it is possible to conclude that, contrarily to that registered for the AA 5182 welds, for this base material the grain size in TMAZ almost do not change with W/v. In fact, the grain size in TMAZ varied from 6·5 to 8 μm, being the lower values registered for the C10 welds performed at 750 rev min^{-1}. Knowing that a fine grained material will recrystallise more rapidly than a coarse grained material,[41] it is reasonable to presume that the rate of recrystallisation during FSW was faster for the AA 5083 alloy than for AA 5182 alloy, leading to a fully recrystallised TMAZ grain structure for the AA 5083 welds, with very similar characteristics independently of the welding conditions.

After a series of 60 hardness measurements, mean hardness values of 71 HV0·05 and 67 HV0·2 were registered for the AA 5182 and AA 5083 base materials respectively. Hardness profiles across the welds demonstrated a hardness increase in the TMAZ, relatively to the base material, for almost all the AA 5182 and AA 5083 welds. The only exception was the C10-1800-160, which was found to be in even match relative to the AA 5182 base material. The average weld hardness values for the different welds are shown in Table 3 and plotted in Fig. 5 against the reciprocal of the square root of the TMAZ grain size $d^{-1/2}$. For comparison, the base material mean hardness values were represented in the graph by using dashed lines.

As it is evident from Fig. 5, the average hardness and grain sizes strongly vary according to the FSW conditions, for the AA 5182 welds, ranging from even match conditions, associated to weld with the larger grain size (10 μm, C10-1800-160 weld), to strong over match, associated to the weld with the smaller grain size (3 μm, S14-1120-640 weld). Comparing the hardness results relative to the AA 5182 welds performed in force control (S14-1120-320F, S14-1120-480 and S14-1120-640), it is also possible to conclude that the hardness of the welds increased with increasing traverse speed. From the graph it is also evident that, despite the hardness and TMAZ grain size strongly depending on the welding conditions, none of the AA 5182 welds was in under match relative to the base material. The relationship between HV and the reciprocal of the square root of the grain size is also plotted in Fig. 5, showing the Hall–Petch relationship applied to AA 5182 results.

Analysing the results relative to the AA 5083 welds in Fig. 5, it is possible to conclude that all the welds were in over match compared to the base material. However, unlike for the AA 5182 alloy, the hardness and grain size

Table 3 Average hardness and grain sizes

|		Hardness/HV	Grain size/μm
AA 5182	Base matertial	71	36·0
	C10-1800-160	71	10·0
	S14-1120-320P	81	7·0
	S14-1120-320F	78	5·0
	S14-1120-480	86	4·0
	S14-1120-640	88	3·0
AA 5083	Base Material	67	18·0
	C10-750-160	77	6·8
	C10-750-250	79	6·5
	C10-1000-160	71	7·3
	C10-1000-250	75	7·2
	C14-750-250	73	7·8
	C14-750-160	72	7·8
	C14-1000-160	72	8·0
	C14-1000-250	71	7·5
	F14-1000-160	77	7·7
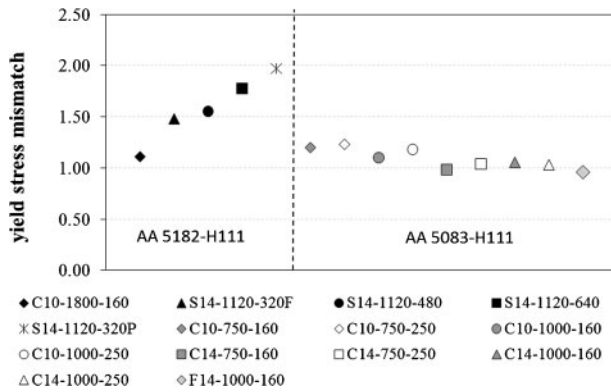
6 Yield strength mismatch of welds relative to base materials

in the TMAZ of the AA 5083 welds varied only slightly with the varying welding conditions. In fact, the TMAZ average hardness values varied from a minimum of 71 HV for the C14 welds to a maximum of 79 HV for the C10-750-250 weld.

In Fig. 6 are resumed the yield mismatch M_y values, calculated as the ratio between the yield stresses in tension of the welds (TMAZ and that of the respective base materials, for all the welds tested in the present work. According to the figure, all the AA 5182 welds, except the C10-1800-180 weld, present strong over match in yield stress relative to the base material. On the other hand, the AA 5083 welds are all almost in even match relative to the base material yield stress, except the C10 welds, performed with 750 rev min^{-1}, which present ~20% yield stress over match. From the results in the graph of Fig. 6, it is also possible to conclude that the yield stress over match level for the welds performed with the scrolled shoulder tool (S14 welds) is much higher than that of the welds performed with the other tools.

Comparing the results of the mechanical characterisation of the S14-1120-320P welds performed in position control with that of the S14 welds performed in load control, it is possible to conclude that the S14-1120-320P welds displayed lower hardness values (*see* Fig. 5) but higher yield stress values (*see* Fig. 6) than all the other S14 welds. These results show that despite the hardness evolution for the AA5182 welds can be described on the basis of grain size and Hall–Petch relation, the yield stress evolution does not obey the same relation rule. In order to analyse the differences in yield strength between the AA 5182 welds, TEM microstructural analysis was performed. For comparison, a micrograph of AA 5182 base material microstructure is shown in Fig. 7a together with TMAZ micrographs of four AA 5182 welds (Fig. 7b–d). The base material micrograph shows an annealed microstructure, free of dislocations and with a large number of precipitates dispersed inside the grains. Similarly, Fig. 7b shows a TEM image of a C10-1800-160 weld nugget, for which an average grain size of 10 μm was registered. A low density of rearranged dislocations can be seen inside the grains, which results in the even matched mechanical properties of these welds compared to the base material. Analysing now the TEM image of the S14-1120-320P weld nugget (Fig. 7c), for which an average grain size of 7 μm and over match mechanical properties were registered, it is possible to observe very small subgrains with an elevated density of dislocations inside it.
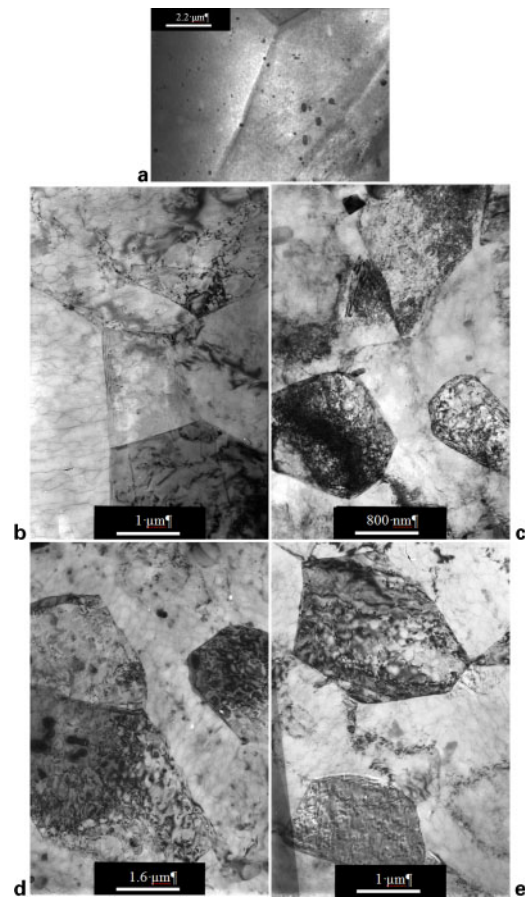
7 Images (TEM) of AA 5182 *a* base material and weld nuggets: *b* C10-1800-180, *c* S14-1120-320P, *d* S14-1120-320F and *e* S14-1120-640

Transmission electron micrographs of S14-1120-320F and S14-1120-640 weld nuggets are also shown in Fig. 7d and *e* respectively. From these pictures it is possible to conclude that these welds are microstructurally similar to the S14-1120-320P welds (Fig. 7c), performed with the same type of tool. However, these welds display a coarser subgrain structure than the S14-1120-320P welds and a lower dislocation density inside the subgrains. Since the S14-1120-320P welds displayed higher yield strength than the other welds (Fig. 6), it is reasonable to assume that the subgrain structure plays a major role in determining the welds strength.

Conclusions

The aim of this investigation was to study the influence of base material properties and process parameters on the properties of 1 mm thick welds in AA 5182-H111 and AA 5083-H111 alloys, produced using the FSW process. As it is clearly stated in the paper introduction, despite several papers had already addressed the mechanical and microstructural characterisation of friction stir welds in aluminium alloys, to the authors' knowledge, only a few of those papers addressed the study of welds in non-heat treatable aluminium alloys, the application of the process in the joining of very thin plates and the influence of process parameters, with special focus on shoulder dimensions and geometry, on weld quality. From the present investigation, where all these aspects were addressed, it is possible to conclude that

1. It is possible to obtain consistently good quality welds in very thin plates under a large range of welding conditions. In fact, hardness and tensile testing of the welds demonstrates that independent of the welding conditions and of the base material, the TMAZ material has at least even matched mechanical properties relative to the base materials.

2. Reducing the heat input during welding, improves the mechanical strength of the welds.

3. The reduction in heat input must be achieved by increasing the traverse speed of the tool, which is of interest in terms of process productivity.

4. The utilisation of small shoulder diameter tools, which also enable to reduce the heat generation, also led to improved weld properties.

5. Scrolled shoulder tools, which induce high deformation rates in the stirred zone, also conducted to improved mechanical strength of the welds.

6. The smaller the initial base material grain size, the more homogeneous the weld properties for different welding conditions.

7. For the AA 5182-H111 alloy, the TMAZ subgrain structure plays a major role in determining welds yield strength.

Acknowledgements

References

1. R. Nandan, T. DebRoy and H. K. D. H. Bhadeshia: 'Recent advances in friction-stir welding – process, weldment structure and properties', *Prog. Mater. Sci.*, 2008, **53**, (6), 980–1023.

2. T. DebRoy and H. Bhadeshia: 'Friction stir welding of dissimilar alloys – a perspective', *Sci. Technol. Weld. Join.*, 2010, **15**, (4), 266–270.

3. P. Alvarez, G. Janeiro, A. A. M. da Silva, E. Aldanondo and A. Echeverría: 'Material flow and mixing patterns during dissimilar FSW', *Sci. Technol. Weld. Join.*, 2010, **15**, 648–653.

4. I. Eberl, C. Hantrais, J. C. Ehrtsrom and C. Nardin: 'Friction stir welding dissimilar alloys for tailoring properties of aerospace parts', *Sci. Technol. Weld. Join.*, 2010, **15**, 699–705.

5. S. M. O. Tavares, R. A. S. Castro, V. Richter-Trummer, P. Vilaça, P. M. G. P. Moreira and P. M. S. T. de Castro: 'Friction stir welding of T-joints with dissimilar aluminium alloys: mechanical joint characterisation', *Sci. Technol. Weld. Join.*, 2010, **15**, 312–318.

6. M. K. Yadava, R. S. Mishra, Y. L. Chen, B. Carlson and G. J. Grant: 'Study of friction stir joining of thin aluminium sheets in lap joint configuration', *Sci. Technol. Weld. Join.*, 2010, **15**, 70–75.

7. M. P. Miles, T. W. Nelson and B. J. Decker: 'Formability and strength of friction-stir-welded aluminum sheets', *Metall. Mater. Trans. A*, 2004, **35A**, (11), 3461–3468.

8. M. P. Miles, T. W. Nelson and D. W. Melton: 'Formability of friction-stir-welded dissimilar-aluminum-alloy sheets', *Metall. Mater. Trans. A*, 2005, **36A**, (12), 3335–3342.

9. I. Shigematsu, Y. J. Kwon, K. Suzuki, T. Imai and N. Saito: 'Joining of 5083 and 6061 aluminum alloys by friction stir welding', *J. Mater. Sci. Lett.*, 2003, **22**, (5), 353–356.

10. M. J. Peel, A. Steuwer and P. J. Withers: 'Dissimilar friction stir welds in AA5083-AA6082. Part II: process parameter effects on microstructure', *Metall. Mater. Trans. A*, 2006, **37A**, 2195–2206.

11. L. E. Murr, Y. Li, R. D. Flores, E. A. Trillo and J. C. McClure: 'Intercalation vortices and related microstructural features in the friction-stir welding of dissimilar metals', *Mater. Res. Innov.*, 1998, **2**, (3), 150–163.

12. M. Peel, A. Steuwer, M. Preuss and P. J. Withers: 'Microstructure, mechanical properties and residual stresses as a function of welding speed in aluminium AA5083 friction stir welds', *Acta Mater.*, 2003, **51**, (16), 4791–4801.

13. G. M. D. Cantin, S. A. David, W. M. Thomas, E. Lara-Curzio and S. S. Babu: 'Friction skew-stir welding of lap joints in 5083-0 aluminium', *Sci. Technol. Weld. Joini.*, 2005, **10**, 268–280.

14. Z. W. Chen, T. Pasang and Y. Qi: 'Shear flow and formation of nugget zone during friction stir welding of aluminium alloy 5083-O', *Mater. Sci. Eng. A*, 2008, **A474**, (1–2), 312–316.

15. T. Hirata, T. Oguri, H. Hagino, T. Tanaka, S. W. Chung, Y. Takigawa and K. Higashi: 'Influence of friction stir welding parameters on grain size and formability in 5083 aluminum alloy', *Mater. Sci. Eng. A*, 2007, **A456**, (1–2), 344–349.

16. S. Hong, S. Kim, C. Lee and S.-J. Kim: 'Fatigue crack propagation behavior of friction stir welded 5083-H32 Al alloy', *J. Mater. Sci.*, 2007, **42**, (23), 9888–9893.

17. H. J. Liu, H. Fujii, M. Maeda and K. Nogi: 'Friction stir welding of AA5083 aluminum alloy', *Trans. Nonferrous Met. Soc. China*, 2003, **13**, (Suppl. 1), 14–17.

18. H. Lombard, D. G. Hattingh, A. Steuwer and M. N. James: 'Effect of process parameters on the residual stresses in AA5083-H321 friction stir welds', *Mater. Sci. Eng. A*, 2009, **A501**, (1–2), 119–124.

19. Y. Sato, S. Park and H. Kokawa: 'Microstructural factors governing hardness in friction-stir welds of solid-solution-hardened Al alloys', *Metall. Mater. Trans. A*, 2001, **32A**, (12), 3033–3042.

20. Y. Uematsu, K. Tokaji, H. Shibata, Y. Tozaki and T. Ohmune: 'Fatigue behaviour of friction stir welds without neither welding flash nor flaw in several aluminium alloys', *Int. J. Fatigue*, 2009, **31**, (10), 1443–1453.

21. C. Zhou, X. Yang and G. Luan: 'Fatigue properties of friction stir welds in Al 5083 alloy', *Scr. Mater.*, 2005, **53**, (10), 1187–1191.

22. D. M. Rodrigues, C. Leitao, R. Louro, H. Gouveia and A. Loureiro: 'High speed friction stir welding of aluminium alloys', *Sci. Technol. Weld. Join.*, 2010, **15**, 676–681.

23. K. Kimapong and T. Watanabe: 'Lap joint of A5083 aluminum alloy and SS400 steel by friction stir welding', *Mater. Trans.*, 2005, **46**, (4), 835–841.

24. F. Sarsılmaz and U. Çaydaş: 'Statistical analysis on mechanical properties of friction-stir-welded AA 1050/AA 5083 couples', *Int. J. Adv. Manuf. Technol.*, 2009, **43**, (3), 248–255.

25. M. Kulekci, A. Şik and E. Kaluç: 'Effects of tool rotation and pin diameter on fatigue properties of friction stir welded lap joints', *Int. J. Adv. Manuf. Technol.*, 2008, **36**, (9), 877–882.

26. Y. S. Sato, Y. Sugiura, Y. Shoji, S. H. C. Park, H. Kokawa and K. Ikeda: 'Post-weld formability of friction stir welded Al alloy 5052', *Mater. Sci. Eng. A*, 2004, **A369**, (1–2), 138–143.

27. Y. J. Kwon, S. B. Shim and D. H. Park: 'Friction stir welding of 5052 aluminum alloy plates', *Trans. Nonferrous Met. Soc. China*, 2009, **19**, s23–s27.

28. S. K. Park, S. T. Hong, J. H. Park, K. Y. Park, Y. J. Kwon and H. J. Son: 'Effect of material locations on properties of friction stir welding joints of dissimilar aluminium alloys', *Sci. Technol. Weld. Join.*, 2010, **15**, 331–336.

29. H.-B. Chen, K. Yan, T. Lin, S.-B. Chen, C.-Y. Jiang and Y. Zhao: 'The investigation of typical welding defects for 5456 aluminum alloy friction stir welds', *Mater. Sci. Eng. A*, 2006, **A433**, (1–2), 64–69.

30. R. W. Fonda, P. S. Pao, H. N. Jones, C. R. Feng, B. J. Connolly and A. J. Davenport: 'Microstructure, mechanical properties, and corrosion of friction stir welded Al 5456', *Mater. Sci. Eng. A*, 2009, **A519**, (1–2), 1–8.

31. A. L. Etter, T. Baudin, N. Fredj and R. Penelle: 'Recrystallization mechanisms in 5251 H14 and 5251 O aluminum friction stir welds', *Mater. Sci. Eng. A*, 2007, **A445–A446**, 94–99.

32. C. Genevois, A. Deschamps and P. Vacher: 'Comparative study on local and global mechanical properties of 2024 T351, 2024 T6 and 5251 O friction stir welds', *Mater. Sci. Eng. A*, 2006, **A415**, (1–2), 162–170.

33. C. Leitao, R. M. Leal, D. M. Rodrigues, A. Loureiro and P. Vilaça: 'Mechanical behaviour of similar and dissimilar AA5182-H111 and AA6016-T4 thin friction stir welds', *Mater. Des.*, 2009, **30**, (1), 101–108.

34. G. Çam, S. Güçlüer, A. Çakan and H. T. Serindag: 'Mechanical properties of friction stir butt-welded Al-5086 H32 plate', *Mater. Werkst.*, 2009, **40**, (8), 638–642.

35. E. Taban and E. Kaluc: 'Comparison between microstructure characteristics and joint performance of 5086-H32 aluminium alloy welded by MIG, TIG and friction stir welding processes', *Kov. Mater.*, 2007, **45**, (5), 241–248.

36. P. Upadhyay and A. P. Reynolds: 'Effects of thermal boundary conditions in friction stir welded AA7050-T7 sheets', *Mater. Sci. Eng. A*, 2010, **A527**, (6), 1537–1543.

37. P. A. Colegrove and H. R. Shercliff: 'CFD modelling of friction stir welding of thick plate 7449 aluminium alloy', *Sci. Technol. Weld. Join.*, 2006, **11**, 429–441.
38. H. B. Schmidt and J. H. Hattel: 'Thermal modelling of friction stir welding', *Scr. Mater.*, 2008, **58**, (5), 332–337.
39. F. J. Humphreys and M. Hatherly: 'Recrystallization and related annealing phenomena'; 2004, New York, Elsevier.
40. R. M. Leal, C. Leitão, A. Loureiro, D. M. Rodrigues and P. Vilaça: 'Material flow in heterogeneous friction stir welding of thin aluminium sheets: effect of shoulder geometry', *Mater. Sci. Eng. A*, 2008, **A498**, (1–2), 384–391.
41. P. A. Colegrove, H. R. Shercliff and R. Zettler: 'Model for predicting heat generation and temperature in friction stir welding from the material properties', *Sci. Technol. Weld. Join.*, 2007, **12**, (4), 284–297.